Science Forum (Journal of Pure and Applied Sciences)

Journal Homepage: https://atbuscienceforum.com.ng/index.php/jpas

Modeling Diphtheria Transmission and Control Strategies in Nigeria Using a Compartmental Model Approach

Fu'ad Muhammad Mukhtar [1,2*], Kazeem Eyitayo Lasisi[2], Bello Abdulkadir Rasheed[2], Hamisu Idi[2], Emmanuel Alphonsus Akpan[3,4], Collins Francis Udom[3], Oghale Gift Otobo[3], Elisha John Inyang[5]

[1]Department of Mathematics, Nigerian Army University, Biu, Nigeria
[2]Department of Statistics, Abubakar Tafawa Balewa University, Bauchi, Nigeria
[3]Department of Basic Sciences, Federal College of Medical Laboratory Science and Technology, Jos, Nigeria
[4]Department of Mathematics, University of Jos, Jos, Nigeria
[5]Department of Statistics, University of Uyo, Uyo, Nigeria

Abstract

Diphtheria remains a significant public health concern in many developing countries, particularly in regions characterized by low immunization coverage and undiagnosed infections. One of the major challenges in controlling the disease is the often-overlooked contribution of asymptomatic individuals, who may silently sustain and propagate transmission within the population. This study develops a deterministic diphtheria vaccine–treatment model to describe the transmission dynamics of diphtheria within the Nigerian population and to evaluate the impact of different vaccination and treatment strategies on disease prevention and control. Model parameters were estimated using reported diphtheria incidence data obtained from the Nigeria Centre for Disease Control covering the period from 1 December 2022 to 31 July 2023. The basic reproduction number, (R_0), was derived analytically, and the estimated mean value of (R_0 = 6.010) indicates sustained endemic transmission and suggests that existing intervention strategies are insufficient to effectively curtail disease spread. Sensitivity analysis identified key epidemiological parameters driving diphtheria transmission dynamics, including the recruitment rate, waning immunity rate from fully vaccinated individuals to the susceptible class, asymptomatic transmission rate, and waning immunity rate from partially vaccinated individuals to susceptibles. The findings underscore the critical need for comprehensive control strategies that extend beyond symptomatic case management. Such strategies should include sustained immunization campaigns, booster vaccination programmes, enhanced surveillance, and targeted interventions aimed at reducing asymptomatic transmission. The proposed model provides valuable quantitative insights for evidence-based diphtheria prevention and control policies, particularly in resource-constrained settings.

Keywords
Diphtheria modeling;
Mathematical modeling;
Infectious diseases;
Epidemiology;
Intervention Strategies;
Basic reproduction number

ISSN 1119-4618 JPAS
1119 4618
Faculty of Science, ATBU Bauchi

Corresponding Author: Fu'ad Muhammad Mukhtar[1]Department of Mathematics, Nigerian Army University, Biu, Nigeria
Email: fuadmmstatistics@gmail.com

Introduction

Diphtheria is an acute bacterial infection that is highly contagious and vaccine-preventable, caused mainly by *Corynebacterium diphtheria* but also by *Corynebacterium ulcerans (1–4).* It spreads between people mainly by direct contact or through the air via respiratory droplets (1,5–7). The disease can affect all age groups; however, unimmunized children are most at risk. Symptoms often come on gradually, beginning with a sore throat and fever. In severe cases, the bacteria produce a poison (toxin) that causes a thick grey or white patch at the back of the throat. This can block the airways, making it hard to breathe or swallow, and also creates a barking cough. The neck may swell in part due to enlarged lymph nodes.

Diphtheria can be fatal in 5-10% of cases, with a higher mortality rate in young children, and its outbreak in Nigeria has maintained a very high risk at the national level. On 27 April 2023, Nigeria reported suspected cases of diphtheria weekly to the WHO. However, between 30 June and 31 August 2023, Nigeria recorded an unusual increase in the number of confirmed diphtheria cases. From 30 June to 31 August 2023, a total of 5898 suspected cases were reported from 59 LGAs in 11 states across the country. The majority (99.4%) of suspected cases were reported from Kano (1816), Katsina (234), Yobe (158), Bauchi (79), Kaduna (45), and Borno (33). Of the cumulative 8353 suspected cases reported since the outbreak was first reported in 2022, 4717 (56.5%) cases were confirmed (lab confirmed (169; 3.6%), epidemiologically linked (117; 2.5%), and clinical compatibility (4431; 93.9%)). While 1857 (22.2%) cases were discarded as not compatible with diphtheria, 1048 (12.5%) cases are pending classification, and 731 (8.8%) cases had an unknown diagnosis.

The case fatality ratio dropped slightly from 6.7% during the last update to 6.1%. Of the 4717 confirmed cases, 3466 (73.5%) were aged 1 – 14 years; of these, 699 were aged 0-4 years, 1505 were aged 5-9 years, and 1262 were aged 10 – 14 years. More than half of the cases (2656; 56.3%) were females. Only 1074 (22.8%) of the confirmed cases were fully vaccinated against diphtheria, 299 (6.3%) were partially vaccinated. More than half of the cases (2801; 59.4%) were unvaccinated.

The occurrence and sporadic spread of diphtheria in Nigeria reflect the inadequacy of national childhood immunization programmes (8). Other factors associated with occurrence of diphtheria outbreaks and high infant mortality include: waning immunity, low vaccine coverage and access, including the need for booster shots over time, prevalence and potential role of asymptomatic carriers, delayed clinical recognition, and absence of treatment with antitoxin and appropriate antibodies (4,7–14).

One useful tool for guiding outbreak control decision-making is mathematical modelling (15–17). Mathematical frameworks segment populations into unique compartments, such as susceptible, infected, and recovered (SIR) and its variants (18–21). These models are essential to simplifying the complexities of disease dynamics (22–24). Also, mathematical models make it easier to understand how infections spread in a community, estimate key parameters, predict how an outbreak might unfold, and provide frameworks for assessing how non-pharmaceutical and pharmaceutical interventions could change the course of an epidemic (25–27).

A growing body of research uses mathematical modelling to enhance the understanding of diphtheria transmission and inform control strategies. Several studies take a detailed approach by dividing the population into multiple compartments representing different stages of infection and awareness. For example, (28) developed an eight-compartment model that distinguishes between aware and unaware exposed individuals, symptomatic and asymptomatic cases, and various stages of monitoring and isolation,

Corresponding Author: Fu'ad Muhammad Mukhtar[1]Department of Mathematics, Nigerian Army University, Biu, Nigeria
Email: fuadmmstatistics@gmail.com

providing a nuanced view of how the disease moves through a community. Similarly, (29) designed a model for the 2017 Jakarta outbreak that includes multiple types of carriers: primary, secondary, and chronic, to capture the significant role of asymptomatic transmission. Other studies focus on how vaccination and waning immunity influence transmission. (30) introduced a five-compartment system that incorporates vaccinated individuals and those with declining immunity, while (31,32) examined the impact of incomplete childhood immunization on diphtheria resurgence.

Some models incorporate broader biological processes, including (4), who analyzed how asymptomatic infection and imperfect vaccination influence outbreaks and identified the minimum vaccination levels needed for eradication. (33,34) applied optimal control theory to explore combinations of vaccination, treatment, and awareness campaigns, showing that integrated interventions offer the best results. Environmental pathways have also attracted attention: (35,36) incorporated environmental contamination and public awareness in their models, highlighting the role of hygiene, disinfection, and booster doses in reducing transmission. One of the most comprehensive approaches is presented by (37), who explicitly modelled both human infection states and the environmental reservoir of *C. diphtheriae*, showing how improved hygiene, increased vaccination, and faster decay of bacteria in the environment can jointly reduce transmission. In a related effort, (38) employed a six-compartment model to evaluate the cost-effectiveness of various interventions, finding that combining prevention with vaccination yields the best value for public health.

Despite the notable progress, it is necessary to incorporate treatment compartments, consider waning immunity, and explore multiple vaccination scenarios for more comprehensive evaluations. Therefore, this study aims to develop a diphtheria vaccine treatment model to describe the transmission dynamics of diphtheria within the Nigerian population and to evaluate the impact of different vaccination scenarios and treatments on preventing and controlling diphtheria.

Materials and Methods

Model Description

This study develops a compartmental deterministic model to explore the transmission dynamics of diphtheria in a population where vaccination, waning immunity, asymptomatic and symptomatic infection, and treatment interventions play significant roles. The model subdivides the total human population into epidemiologically distinct compartments, including Susceptible (unvaccinated) (S_U), making up of individuals who are unvaccinated and lose immunity due to vaccine ineffectiveness and waning over time. Fully vaccinated compartment (V_F) consisting of individuals who have completed the primary vaccination program (3 doses of DTP).

The partially vaccinated compartment (V_P)comprises individuals who lose immunity due to waning and do not receive the full 3 doses of DTP. Exposed (E) individuals are exposed to diphtheria but are not yet infectious. The Asymptomatic infected compartment (I_A) consists of individuals who have diphtheria without symptoms but can still spread the disease. The Symptomatic infected compartment (I_S) comprises individuals who have diphtheria with symptoms and can spread the disease to others. The Treated (T) compartment comprises individuals receiving medical treatment for diphtheria. The Recovered (R) compartment comprises individuals who have recovered from diphtheria and have developed immunity. Recovered (R) are individuals who recovered from the diphtheria disease and have developed immunity.

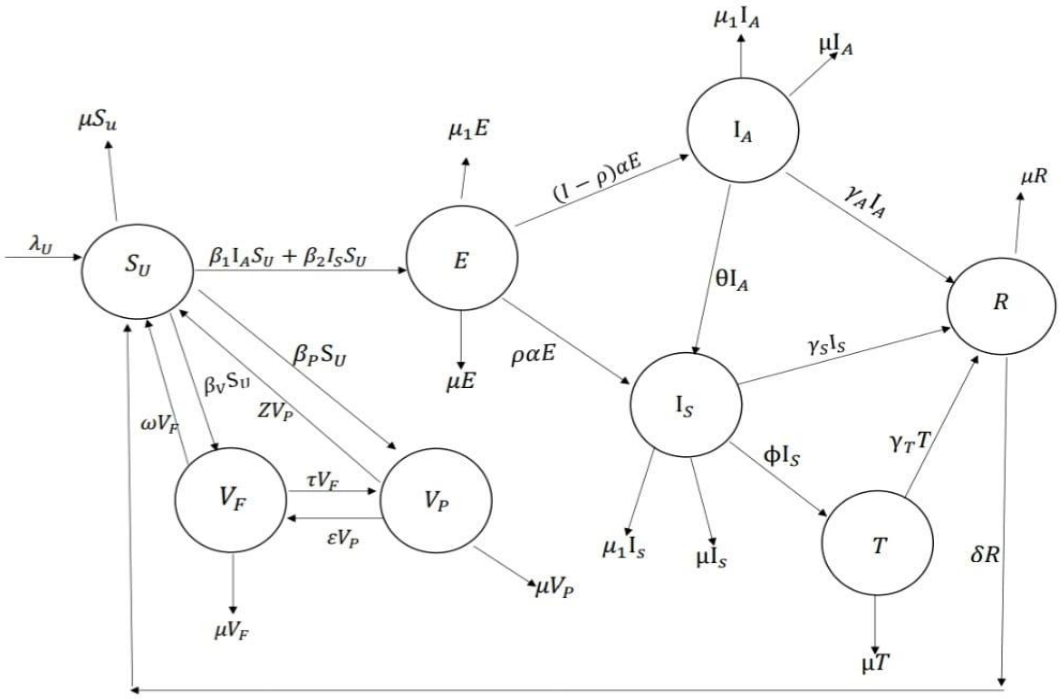

Figure1: Schematic Diagram of the Model

Based on the model development description in 2.1, the schematic diagram in Figure 2, and the model assumptions:

(1) Every child is born susceptible, vulnerable if unvaccinated, and exposed to diphtheria.
(2) The level of immunity wanes over time (for calculation, we assume 2 years and 5 months).
(3) Over time, the effectiveness of the vaccine gradually diminishes leading to reduced protection against diphtheria (for calculation, we assume 2 years and 5 months).
(4) Exposed individuals may not show signs of illness but can still be infectious.
(5) Asymptomatic infected individuals play a significant role in the transmission of diphtheria.
(6) Symptomatic individuals are highly contagious and can easily spread diphtheria.
(7) Individuals with symptoms of diphtheria should be diagnosed and treated.
(8) Infected individuals can recover from illness naturally and can die from illness.
(9) Recovered individuals who developed immunity can lose the immunity and become Susceptible.

Based on the stated assumptions, the following model equations are derived.

$$\frac{dS_U}{dt} = \lambda_u - (\beta_1 I_A + \beta_2 I_S)S_U + \delta R + \omega V_F + zV_P - (\beta_V + \beta_P + \mu)S_U \quad (1)$$

$$\frac{dV_F}{dt} = \beta_V S_U + \varepsilon V_p - (\omega + \tau + \mu)V_F \quad (2)$$

$$\frac{dV_P}{dt} = \beta_P S_U + \tau V_F - (z + \varepsilon + \mu)V_P \quad (3)$$

$$\frac{dE}{dt} = (\beta_1 I_A + \beta_2 I_S)S_U - [(1-\rho)\alpha + \rho\alpha + \mu_1 + \mu]E \quad (4)$$

$$\frac{dI_A}{dt} = (1-\rho)\alpha E - (\theta + \mu_1 + \mu + \gamma_A)I_A \quad (5)$$

$$\frac{dI_S}{dt} = \rho\alpha E + \theta I_A - (\gamma_S + \mu_1 + \mu + \phi)I_S \quad (6)$$

$$\frac{dT}{dt} = \phi I_S - (\gamma_T + \mu)T \quad (7)$$

$$\frac{dR}{dt} = \gamma_A I_A + \gamma_S I_S + \gamma_T T - (\delta + \mu)R \quad (8)$$

$$\frac{dN}{dt} = \frac{dS_U}{dt} + \frac{dV_F}{dt} + \frac{dV_P}{dt} + \frac{dE}{dt} + \frac{dI_A}{dt} + \frac{dI_S}{dt} + \frac{dT}{dt} + \frac{dR}{dt} = \lambda_u + \mu N.$$

Basic Properties

Positivity of the Solution

Every epidemiological rate in the model is assumed strictly positive and finite. We want to show that equations (1) to (8) are non-negative always, for all t ≥ 0.

Theorem 1:

let $\Psi = \begin{Bmatrix} (S_U, V_F, V_P, E, I_A, I_S, T, R) \in \Re_+^8, S_U(0) > 0, V_F(0) > 0, \\ V_P(0) > 0, E(0) > 0, \\ I_A(0) > 0, I_S(0) > 0, T(0) > 0, R(0) > 0 \\ S_U + V_F + V_P + E + I_A + I_S + T + R \leq \frac{\lambda_u}{\mu} \end{Bmatrix}$ (9)

Then the solution of $\{S_U(t), V_F(t), V_P(t), E(t), I_A(t), I_S(t), T(t), R(t)\}$ are positive for all $t \geq 0$.

Proof:

Applying the method used by Wiah (39),

we have

$k_1 = (\beta_V + \beta_P + \mu)$,$k_2 = (1-\rho)\alpha + \rho\alpha + \mu_1 + \mu$, $k_3 = \theta + \mu_1 + \mu + \gamma_A$, $k_4 = \gamma_S + \mu_1 + \mu + \phi$,

$k_5 = \delta + \mu$, $k_6 = \gamma_T + \mu$, $k_7 = \omega + \tau + \mu$, $k_8 = z + \varepsilon + \mu$.

From the susceptible population, we integrate by separation of parameters and find the integrating factor, we get

$\frac{dS_U}{dt} = \lambda_u - (\beta_1 I_A + \beta_2 I_S)S_U + \delta R + \omega V_F + zV_P - (\beta_V + \beta_P + \mu)S_U$

$\frac{dS_U}{dt} \geq \lambda_u - k_1 S_U = \frac{dS_U}{S_U} \geq -k_1 dt = \int \frac{dS_U}{S_U} \geq \int -k_1 dt = S_U(t) \geq S_U(0)e^{-k_1 t} \geq 0.$

From the Fully Vaccinated population, repeating the same procedure as above, we get

$\frac{dV_F}{dt} = \beta_V S_U + \varepsilon S_P - k_7 V_F \rightarrow \frac{dV_F}{dt} \geq -k_7 V_F \rightarrow \frac{dV_F}{V_F} \geq -k_7 dt = \int \frac{dV_F}{V_F} \geq \int -k_7 dt \quad = V_F(t) \geq V_F(0)e^{-k_7 t} \geq 0.$

From the Partially Vaccinated population

$\frac{dV_P}{dt} = \beta_P S_U + \tau V_F - k_8 V_P \rightarrow \frac{dV_P}{dt} \geq -k_8 V_P \rightarrow \frac{dV_P}{V_P} \geq -k_8 dt \rightarrow \int \frac{dV_P}{V_P} \geq \int -k_8 dt$

$= V_P(t) \geq V_P(0)e^{-k_8 t} \geq 0.$

From the Exposed population

$\frac{dE}{dt} = (\beta_1 I_A + \beta_2 I_S)S_U - k_2 E \rightarrow \frac{dE}{dt} \geq -k_2 E \rightarrow \frac{dE}{E} \geq -k_2 dt \rightarrow \int \frac{dE}{E} \geq \int -k_2 dt$

$= E(t) \geq E(0)e^{-k_2 t} \geq 0.$

From the Asymptomatic infected population

$\frac{dI_A}{dt} = (1-\rho)\alpha E - k_3 I_A \rightarrow \frac{dI_A}{dt} \geq -k_3 I_A \rightarrow \frac{dI_A}{I_A} \geq -k_3 dt \rightarrow \int \frac{dI_A}{I_A} \geq \int -k_3 dt =$

$I_A(t) \geq I_A(0)e^{-k_3 t} \geq 0.$

From the Symptomatic Infected population

$\frac{dI_S}{dt} = \rho\alpha E + \theta I_A - k_4 I_S \rightarrow \frac{dI_S}{dt} \geq -k_4 I_S \rightarrow \frac{dI_S}{I_S} \geq -k_4 dt \rightarrow \int \frac{dI_S}{I_S} \geq \int -k_4 dt =$

$I_S(t) \geq I_S(0)e^{-k_4 t} \geq 0.$

From the Treated population

$\frac{dT}{dt} = \phi I_S - k_6 T \rightarrow \frac{dT}{dt} \geq -k_6 T \rightarrow \frac{dT}{T} \geq -k_6 dt \rightarrow \int \frac{dT}{T} \geq \int -k_6 dt =$

$T(t) \geq T(0)e^{-k_6 t} \geq 0$

From the recovered population

$\frac{dR}{dt} = \gamma_A I_A + \gamma_S I_S + \gamma_T T - k_5 R \rightarrow \frac{dR}{dt} \geq -k_5 R \rightarrow \frac{dR}{R} \geq -k_5 dt \rightarrow \int \frac{dR}{R} \geq \int -k_5 dt =$

$R(t) \geq R(0)e^{-k_5 t} \geq 0$

Therefore $S_U, V_F, V_P, E, I_A, I_S, T, R$ remains positive at every given time. The solutions of the model equations (1) to (8) are all positive. Hence, the model is valid.

Equilibrium State

We set the rate of change to zero at equilibrium. That is, setting all of the equations in the system (1) to zero, so that at equilibrium

$\frac{dS_U}{dt} = \frac{dV_F}{dt} = \frac{dV_P}{dt} = \frac{dE}{dt} = \frac{dI_A}{dt} = \frac{dI_S}{dt} = \frac{dT}{dt} = \frac{dR}{dt} = 0.$

Disease-Free Equilibrium

A disease-free equilibrium is reached in the model system (1-8) when infectious classes are zero. By putting the right-hand sides of each equation in system (1-8) to zero, the disease-free equilibrium can be determined. Equations solved yield the disease-free equilibrium in equation (10)

$$\begin{pmatrix} S_U^0 \\ V_F^0 \\ V_P^0 \\ E^0 \\ I_A^0 \\ I_S^0 \\ T^0 \\ R^0 \end{pmatrix} = \begin{pmatrix} \frac{\lambda_u(\tau\varepsilon - k_7k_8)}{k_1(\tau\varepsilon - k_7k_8)+\omega(\varepsilon\beta_p+\beta_vk_8)+z(\tau\beta_v+\beta_pk_7)} \\ \frac{\lambda_u(\tau\varepsilon - k_7k_8)(\varepsilon\beta_P-\beta_Vk_8)}{k_1(\tau\varepsilon - k_7k_8)+\omega(\varepsilon\beta_p+\beta_vk_8)+z(\tau\beta_v+\beta_pk_7)(\varepsilon\tau-k_7k_8)} \\ \frac{\lambda_u(\tau\varepsilon - k_7k_8)(\tau\beta_v+\beta_Pk_7)}{k_1(\tau\varepsilon - k_7k_8)+\omega(\varepsilon\beta_p+\beta_vk_8)+z(\tau\beta_v+\beta_pk_7)(\varepsilon\tau-k_7k_8)} \\ 0 \\ 0 \\ 0 \\ 0 \\ 0 \end{pmatrix}. \quad (10)$$

Local Stability of Disease-Free Equilibrium State

We investigate the local stability of the equilibrium points using the theorem below:

Theorem 2: The disease-free equilibrium of the model equations (1)-(8) is locally asymptotically stable if $R_0 < 1$.

Proof:

Linearizing the model equations (1)-(8) at any arbitrary equilibrium point (E^*). We also evaluated the Jacobian at the disease-free equilibrium to determine the local stability of the system and obtained;

$$J(E^0) = \begin{pmatrix} -k_1 & \omega & z & 0 & -\beta_1S_U^0 & -\beta_2S_U^0 & 0 & \delta \\ \beta_v & -k_7 & \varepsilon & 0 & 0 & 0 & 0 & 0 \\ \beta_p & \tau & k_8 & 0 & 0 & 0 & 0 & 0 \\ 0 & 0 & 0 & -k_2 & \beta_1S_U^0 & \beta_2S_U^0 & 0 & 0 \\ 0 & 0 & 0 & (1-\rho)\alpha & -k_3 & 0 & 0 & 0 \\ 0 & 0 & 0 & \rho\alpha & \theta & -k_4 & 0 & 0 \\ 0 & 0 & 0 & 0 & 0 & \phi & -k_6 & 0 \\ 0 & 0 & 0 & 0 & \gamma_AI_A & \gamma_S & \gamma_T & -k_5 \end{pmatrix}. \quad (11)$$

Using elementary row transformation, the matrix above becomes $J(E^0) =$

$$\begin{pmatrix} -k_1 & \omega & z & 0 & -\beta_1S_U^0 & -\beta_2S_U^0 & 0 & \delta \\ 0 & a_1 & a_2 & 0 & -a_4 & -a_5 & 0 & a_6 \\ 0 & 0 & -a_3 & 0 & a_7 & a_8 & 0 & -a_9 \\ 0 & 0 & 0 & -k_2 & \beta_1S_U^0 & \beta_2S_U^0 & 0 & 0 \\ 0 & 0 & 0 & 0 & -a_{10} & -a_{11} & 0 & 0 \\ 0 & 0 & 0 & 0 & \theta & -a_{12} & 0 & 0 \\ 0 & 0 & 0 & 0 & 0 & 0 & -k_6 & 0 \\ 0 & 0 & 0 & 0 & 0 & 0 & 0 & -k_5 \end{pmatrix}, \quad (12)$$

where

$a_1 = \frac{\omega\beta_v - k_1k_4}{k_1}, a_2 = \frac{z\beta_v - \varepsilon k_1}{k_1}, a_3 = \frac{\tau z\beta_v + \tau\varepsilon k_1 + \omega\varepsilon\beta_p + \omega\beta_vk_8 + z\beta_pk_7 + k_1k_7k_8}{\omega\beta_v + k_1k_7},$

$a_4 = \frac{\beta_v\beta_1S_U^0}{k_1}, a_5 = \frac{\beta_v\beta_2S_U^0}{k_1}, a_6 = \frac{\beta_v\delta}{k_1}, a_7 = \frac{\beta_1S_U^0(\tau\beta_v+\beta_pk_7)}{\omega\beta_v+k_1k_7}, a_8 = \frac{\beta_2S_U^0(\tau\beta_v+\beta_pk_7)}{\omega\beta_v+k_1k_7}, a_9 = \frac{\delta(\tau\beta_v+\beta_pk_7)}{\omega\beta_v\mp k_7},$

$a_{10} = \frac{\alpha\rho\beta_1 S_U - \alpha\beta_1 S_U^0 - k_2 k_3}{k_2}$, $a_{11} = \frac{(-1+\rho)\alpha\beta_2 S_U}{k_2}$,

$a_{12} = \frac{\alpha\rho\theta\beta_2 S_U^0 + \alpha\rho\beta_1 S_U^0 k_4 - \alpha\theta\beta_2 S_U^0 - \alpha\beta_1 S_U^0 k_4 + \alpha\rho\beta_2 S_U^0 k_3 - k_2 k_3 k_4}{\alpha\rho\beta_1 S_U^0 - \alpha\beta_1 S_U^0 - k_2 k_3}$,

After computing the characteristic equations of the upper triangular Jacobian matrix, the eigenvalues are:

$\lambda_1 = -k_6 < 0, \lambda_2 = -k_5 < 0, \lambda_3 = -k_2 < 0, \lambda_4 = -k_1 < 0, \lambda_5 = -\frac{\alpha\rho\beta_1 S_U^0 - \alpha\beta_1 S_U^0 - k_2 k_3}{k_2} < 0,$

$\lambda_6 = \frac{k_4(\alpha\rho\beta_2 k_3 + \alpha\beta_1 k_4 + \alpha\theta\beta_2 - \alpha\rho\beta_1 k_4 - \alpha\rho\theta\beta_2 + \alpha\beta_1(1-\rho)k_4 + \alpha\beta_2(\rho k_3 + \theta - \rho\theta))}{\alpha\rho\beta_1 k_4 - \alpha\beta_1 k_4 - \alpha\beta_1(1-\rho)k_4 + \alpha\beta_2(\rho k_3 + \theta - \rho\theta)}$,

$\lambda_7 = -\frac{\omega\beta_v + k_1 k_7}{k_1} < 0, \lambda_8 = -\frac{\tau z\beta_v + \tau\varepsilon k_1 + \omega\varepsilon\beta_p + \omega\beta_p k_8 + z\beta_p k_7 + k_1 k_7 k_8}{\omega\beta_v + k_1 k_7}$.

For λ_6 to be negative, then

$$\frac{k_4(\alpha\rho\beta_2 k_3 + \alpha\beta_1 k_4 + \alpha\theta\beta_2 - \alpha\rho\beta_1 k_4 - \alpha\rho\theta\beta_2 + \alpha\beta_1(1-\rho)k_4 + \alpha\beta_2(\rho k_3 + \theta - \rho\theta))}{\alpha\rho\beta_1 k_4 - \alpha\beta_1 k_4 - \alpha\beta_1(1-\rho)k_4 + \alpha\beta_2(\rho k_3 + \theta - \rho\theta)} < 0,$$

$\frac{\alpha(\rho\beta_2 k_3 + \beta_1 k_4 + \theta\beta_2 - \rho\beta_1 k_4 - \rho\theta\beta_2)}{\alpha\beta_1(1-\rho)k_4 + \alpha\beta_2(\rho k_3 + \theta - \rho\theta)} < 1 \Rightarrow R_0 < 1$. This implies that, $\lambda_6 < 0$ if $R_0 < 1$,

the disease-free equilibrium E^o of the equations (1) - (8) is locally asymptotically stable (LAS) if $R_0 < 1$.

Endemic equilibrium point (EEP)

This is the state in which the infectious classes (E, I_A, I_S) are not zero. The Endemic equilibrium can be determined, and the equation solved yields EEP below:

$S_U^{**} = \frac{k_2 k_3 k_4}{\alpha(\beta_1 k_4 + \theta\beta_2 + \rho\beta_2 k_3 - \rho\theta\beta_2 - \rho\beta_1 k_4)}$.

$V_F^{**} = \left(\frac{k_8\beta_V + \varepsilon\beta_P}{\tau\varepsilon - k_7 k_8}\right) S_U^{**}$.

$V_P^{**} = \left(\frac{(k_7 k_8 - \tau)\beta_P + \tau(k_8\beta_V + \varepsilon\beta_P)}{(\tau\varepsilon - k_7 k_8)}\right) S_U^{**}$.

$E^{**} = \frac{k_3 A_1}{(1-\rho)\alpha}$.

$I_A^{**} = \frac{\begin{pmatrix} (\lambda_{IA}+\lambda_{IS})(k_7 k_8 - \tau)k_8 - \omega k_8(k_8\beta_V + \varepsilon\beta_P) \\ -z\left((k_7 k_8 - \tau)\beta_P + \tau\begin{pmatrix} k_8\beta_V + \varepsilon\beta_P + \\ k_1 k_8(k_7 k_8 - \tau) \end{pmatrix}\right) \\ -\lambda_u(k_7 k_8 - \tau)k_8 \end{pmatrix} k_4 k_5 k_6 (1-\rho)\alpha}{\delta k_8(k_7 k_8 - \tau)\begin{pmatrix} \gamma_A(k_4 k_6(1-\rho)\alpha) + \gamma_S k_6(\rho\alpha k_3 + \theta(1-\rho)\alpha) \\ +\gamma_T(\phi(\rho\alpha k_3 + \theta(1-\rho)\alpha)) \end{pmatrix}}$.

$I_S^{**} = \left(\frac{\rho\alpha k_3 + \sigma(1-\rho)\alpha}{k_4(1-\rho)\alpha}\right) A_1$.

$T^{**} = \phi\left(\frac{\rho\alpha k_3 + \sigma(1-\rho)\alpha}{k_4 k_8(1-\rho)\alpha}\right) A_1$.

$R^{**} = \frac{(\lambda_{IA}+\lambda_{IS})(k_7 k_8 - \tau)k_8 - \omega k_8(k_8\beta_V + \varepsilon\beta_P) - z\left((k_7 k_8 - \tau)\beta_P + \tau(k_8\beta_V + \varepsilon\beta_P + k_1 k_8(k_7 k_8 - \tau))\right) - \lambda_u(k_7 k_8 - \tau)k_8}{\delta(k_7 k_8 - \tau)k_8}$.

where $A_1 = I_A$.

Stability Analysis of Endemic Equilibrium State

An important criterion by Routh-Hurwitz gives the necessary and sufficient conditions for all roots of the characteristic equation (with real coefficients) to lie in the left half of the complex plane. In other words, all the roots of the polynomial are negative or have real roots if and only if the determinant of all Hurwitz matrices is positive.

Theorem 3 (Routh-Hurwitz Conditions)

Let $J = \begin{pmatrix} f_x(x_*, y_*) & f_y(x_*, y_*) \\ g_x(x_*, y_*) & g_y(x_*, y_*) \end{pmatrix}$ be the Jacobian matrix of the non-linear system

$\frac{dx}{dt} = f(x, y)$, $\frac{dy}{dt} = g(x, y)$

Evaluated at the critical point (x_*, y_*), then the critical point (x_*, y_*);

1. Is locally asymptotically stable if trace (J)<0 and determinant>0

2. Is stable but not asymptotically stable if trace (J)=0 and determinant (J)>0
3. Is unstable if either trace (J)>0 or determinant (J)<0

Differentiating and finding the trace and determinant, we get

$$J(E^*) = \begin{pmatrix} -(c_1+k_1) & \omega & z & 0 & -\beta_1 & -\beta_2 & 0 & \delta \\ \beta_v & -k_7 & \varepsilon & 0 & 0 & 0 & 0 & 0 \\ \beta_p & \tau & k_8 & 0 & 0 & 0 & 0 & 0 \\ c_1 & 0 & 0 & -k_2 & \beta_1 & \beta_2 & 0 & 0 \\ 0 & 0 & 0 & (1-\rho)\alpha & -k_3 & 0 & 0 & 0 \\ 0 & 0 & 0 & \rho\alpha & \theta & -k_4 & 0 & 0 \\ 0 & 0 & 0 & 0 & 0 & \phi & -k_6 & 0 \\ 0 & 0 & 0 & 0 & \gamma_A & \gamma_S & \gamma_T & -k_5 \end{pmatrix}, \quad (13)$$

where.$c_1 = \beta_1 I_A^{**} + \beta_2 I_S^{**}$

The Trace is

$$-\left(A\beta_1 + \frac{z_1}{k_4(1-\rho)\alpha} + k_1 + k_7 - k_8 + k_2 - k_3 + k_4 + k_5 + k_6\right), \quad (14)$$

where $z_1 = \frac{(\rho\alpha k_3 + \sigma(1-\rho)\alpha)A\beta_2}{k_4(1-\rho)\alpha}$.

The determinant is

$$-\alpha\omega\rho\theta S_U^{**}\beta_2 k_5 k_6(\varepsilon\beta_P - \beta_V k_8) + \alpha\omega\rho\varepsilon\beta_P S_U^{**} k_5 k_6(\beta_2 k_3 - \beta_1 k_4) + \propto \omega\rho S_U^{**}\beta_V k_5 k_6 k_8(\beta_1 k_4 - \beta_2 k_3) - \alpha\rho\tau\theta S_U^{**}\beta_2 k_5 k_6(z\beta_V + \varepsilon k_1) - \alpha\rho\tau z\beta_V S_U^{**} k_5 k_6(\beta_2 k_4 - \beta_1 k_3) - \alpha\rho\tau\varepsilon\beta_V S_U^{**} k_1 k_5 k_6(\beta_1 k_4 - \beta_2 k_3) - \alpha\rho\theta z S_U^{**}\beta_2 k_5 k_6(\beta_P k_7 - k_1 k_8) - \alpha\rho z S_U^{**}\beta_P k_5 k_6 k_7(\beta_1 k_4 - \beta_2 k_3) - \alpha\rho S_U^{**}\beta_1 k_1 k_4 k_5 k_6 k_7 k_8 + \alpha\rho S_U^{**}\beta_2 k_1 k_3 k_5 k_6 k_7 k_8 - \alpha\delta\phi\rho\tau\varepsilon c_1\gamma_T(\theta - k_3 + \theta k_7 k_8) + \alpha\delta\phi\rho c_1\gamma_T k_3 k_7 k_8 - \alpha\delta\rho\tau\varepsilon c_1 k_6(\theta\gamma_S + \gamma_A - \gamma_S k_3) - \alpha\delta\rho c_1 k_6 k_7 k_8(\theta\gamma_S + \gamma_A k_4 - \gamma_S k_3) + \alpha\omega\theta\varepsilon S_U^{**}\beta_2\beta_P k_5 k_6 - \alpha\omega\theta S_U^{**}\beta_2\beta_V k_5 k_6 k_8 + \alpha\omega\varepsilon S_U^{**}\beta_1\beta_P k_4 k_5 k_6 - \alpha\omega S_U^{**}\beta_1\beta_V k_4 k_5 k_6 k_8 + \alpha\tau\theta z S_U^{**}\beta_2\beta_V k_5 k_6 + \alpha\tau\theta\varepsilon S_U^{**}\beta_2 k_1 k_5 k_6 + \alpha\tau z S_U^{**}\beta_1\beta_V k_4 k_5 k_6 + \alpha\tau\varepsilon S_U^{**}\beta_1 k_1 k_4 k_5 k_6 + \alpha\theta z S_U^{**}\beta_2\beta_P k_5 k_6 k_7 + \alpha\theta S_U^{**}\beta_2 k_1 k_5 k_6 k_7 k_8 + \alpha z S_U^{**}\beta_1\beta_P k_4 k_5 k_6 k_7 + \alpha S_U^{**}\beta_1 k_1 k_4 k_5 k_6 k_7 k_8 + \alpha\delta\tau c_1(\phi\varepsilon\theta\gamma_T + \phi\theta\gamma_T k_7 k_8 + \theta\varepsilon\gamma_S k_6 + \varepsilon\gamma_A k_4 k_6) + \alpha\delta c_1 k_6 k_7 k_8(\theta\gamma_S + \gamma_A k_4) - \omega\varepsilon\beta_P k_2 k_3 k_4 k_5 k_6 + \omega\beta_V k_2 k_3 k_4 k_5 k_6 k_8 - \tau z\beta_V k_2 k_3 k_4 k_5 k_6 - \tau\varepsilon c_1 k_2 k_3 k_4 k_5 k_6 - \tau\varepsilon k_1 k_2 k_3 k_4 k_5 k_6 - z\beta_p k_2 k_3 k_4 k_5 k_6 k_7 - c_1 k_2 k_3 k_4 k_5 k_6 k_7 k_8 - k_1 k_2 k_3 k_4 k_5 k_6 k_7 k_8$$

The endemic equilibrium is locally asymptotically stable according to the first stability criterion as stated in the conditions for stability earlier, since the determinant is positive and the trace of the Jacobian is negative.

Basic Reproduction Number, R_0

The basic reproduction number (R_0) is often described as the mean value of the secondary cases resulting from a typical primary case in a completely susceptible population. R_0 is an important quantity in infectious disease systems epidemiology, which acts as a threshold value that controls the local stability of the disease-free equilibrium (40). If the reproduction ratio is greater than one, the disease will spread throughout the entire population; if it is less than one, the disease will die out over time. The basic reproduction number determines the direction of the disease (37). E, I_A, I_s and the expected secondary infections depend on these classes. The rate of appearance of new infections in compartments I is given by the matrix.

$$F = \begin{pmatrix} 0 & \beta_1 S_U^\circ & \beta_2 S_U^\circ \\ 0 & 0 & 0 \\ 0 & 0 & 0 \end{pmatrix}, \; V = \begin{pmatrix} k_2 & 0 & 0 \\ -(1-\rho)\alpha & k_3 & 0 \\ -\rho\alpha & -\theta & k_4 \end{pmatrix}, V^{-1} = \begin{pmatrix} \frac{1}{k_2} & 0 & 0 \\ \frac{-(1-\rho)\alpha}{k_2 k_3} & \frac{1}{k_3} & 0 \\ \frac{-\alpha(\theta+\rho k_3+\rho\theta)}{k_2 k_3 k_4} & \frac{\theta}{k_3 k_4} & \frac{1}{k_4} \end{pmatrix},$$

we calculate the eigenvalues to determine the basic reproductive number R_0. Taking the dominant eigenvalue of the matrix FV^{-1} and computing $|A - \lambda I| = 0$ gives

$$FV^{-1} = \begin{pmatrix} \frac{\beta_1 S_U^0(1-\rho)\alpha}{k_2 k_3} - \frac{\beta_2 \alpha S_U^0(\rho k_3 - \rho\theta + \theta)}{k_2 k_3 k_4} - \lambda & \frac{\beta_1 S_U^0}{k_3} + \frac{\beta_2 S_U^0 \theta}{k_3 k_4} & \frac{\beta_2 S_U^0}{k_4} \\ 0 & 0-\lambda & 0 \\ 0 & 0 & 0-\lambda \end{pmatrix} = 0$$

$\lambda_1 = \frac{\lambda_u(\tau\varepsilon - k_7 k_8)\alpha(\beta_2\rho k_3 + \theta\beta_2 + \beta_1 k_4 - \rho\beta_1 k_4 - \rho\theta\beta_2)}{(k_1(\tau\varepsilon - k_7 k_8) + \omega(\varepsilon\beta_p + \beta_v k_8) + z(\tau\beta_v + \beta_p k_7))k_2 k_3 k_4}$, $\lambda_2 = 0$, $\lambda_3 = 0$.

Clearly, the dominant eigenvalue, λ_1, is taken to be the basic reproduction number. Therefore

$R_0 = \frac{\lambda_u(\tau\varepsilon - k_7 k_8)\alpha(\beta_2\rho k_3 + \theta\beta_2 + \beta_1 k_4 - \rho\beta_1 k_4 - \rho\theta\beta_2)}{(k_1(\tau\varepsilon - k_7 k_8) + \omega(\varepsilon\beta_p + \beta_v k_8) + z(\tau\beta_v + \beta_p k_7))k_2 k_3 k_4}$. (16)

Substituting for $k_1, k_2, k_3, k_4, k_7, k_8$, we have

$$R_0 = \frac{\lambda_u(\tau\varepsilon - (\omega+z+\mu)(z+\varepsilon+\mu))\alpha(\beta_2\rho(\theta+\mu_1+\mu+\gamma_A) + \theta\beta_2 + \beta_1(\phi+\mu_1+\mu+\gamma_S) - \rho\beta_1(\phi+\mu_1+\mu+\gamma_S) - \rho\theta\beta_2)}{((\beta_V+\beta_P+\mu)(\tau\varepsilon - (\tau\varepsilon - (\omega+z+\mu)(z+\varepsilon+\mu)) + \omega(\varepsilon\beta_p + \beta_v(z+\varepsilon+\mu)) + z(\tau\beta_v + \beta_p(\omega+z+\mu)))} \over ((1-\rho)\alpha + \rho\alpha + \mu_1 + \mu)(\theta+\mu_1+\mu+\gamma_A)(\phi+\mu_1+\mu+\gamma_S)}.$$ (17)

Sensitivity Analysis for the Parameters Using Basic Reproductive Number

Sensitivity Analysis (SA) highlights the significance of model parameters by revealing their relative influence on the dynamics of diphtheria. It is a crucial tool for identifying key factors that drive disease transmission, offering valuable insights for implementing timely and effective intervention strategies (41). According to (42), Sensitivity analysis is widely employed to assess the reliability of model predictions by evaluating their dependence on parameter values. Omitting this crucial step in modeling is often considered misleading, as it undermines the credibility and accuracy of the results. Sensitivity indices measure the relative changes in a variable when a parameter changes (43). In particular, the normalized forward sensitivity index expresses the proportional change in a given variable relative to changes in a specific parameter. When the variable is a differentiable parameter function, the sensitivity index can also be defined through partial derivatives, providing a rigorous mathematical framework for assessing parameter sensitivity.

$S_\psi^{R_0} = \frac{\partial R_0}{\partial \psi} \times \frac{\psi}{R_0}$, (18)

where $\psi \in Q = \{\beta_1, \beta_2, \beta_{V,}\beta_{P,}\gamma_A, \gamma_s, \phi, \mu, \rho, \theta, \mu_1, z, \alpha, \varepsilon, \lambda_U, \omega, \tau\}$

and R_0 is the basic reproductive number as obtained in (17).

The interpretation of the sensitivity analysis of our basic reproduction number is as follows. Parameters with negative sensitivity indices reduce the burden of diphtheria in the community when their values increase (indicating that the disease's basic reproduction number decreases as their parameter values increase). Parameters with positive sensitivity indices play an important role in the spread of diphtheria in the community, as their values increase (secondary infections increase). Therefore, to minimize the disease in the community, it is vital to decrease the positive indices and increase the negative indices.

Variables and Parameter Values Estimations

The values for the population-dependent parameters of the model are presented in Table 1.

Table 1: Values for the Population-Dependent Parameter of the Model

Description	Variables	Values	Source
Susceptible (Unvaccinated) population	S_U	1787416	(2)
Fully vaccinated population	V_F	2306303	(2)
Partially vaccinated population	V_p	1410329	(2)

Exposed population	E	20725	(2)
Asymptomatic infected population	I_A	1251	(2)
Symptomatic infected population	I_S	3466	(2)
Treated population	T	214	(2)
Recovered population	R	1000	Assumed

The values in Table 2 were obtained from either self-estimation or authors who have conducted similar research on diphtheria infection.

Table 2: Estimation of Parameters

Parameters	Value	Reference	Description
λ_U	100	(35)	Recruitment rate
μ	0.0000491431	(35)	Natural death rate
μ_1	0.011	Calculated	Diphtheria-induced death rate
β_1	**0.201***	Estimated	Asymptomatic infection transmission rate
β_2	**0.0709***	Estimated	Symptomatic infection transmission rate
β_V	0.95	(2)	The rate at which susceptible individuals become fully vaccinated
β_P	**0.503***	Estimated	The rate at which susceptible individuals become partially vaccinated
ω	**0.0114***	Estimated	The rate at which fully vaccinated individuals become susceptible
z	**0.00777***	Estimated	The rate at which partially vaccinated individuals become susceptible
τ	**0.0289***	Estimated	The rate at which individuals go from being fully vaccinated to partially vaccinated
ε	**0.0707***	Estimated	The rate at which partially vaccinated individuals become fully vaccinated
ρ	0.2	(35)	Proportion of infectious population
α	**0.146***	Estimated	Rate of progression from the exposed class to either the asymptomatic compartment or the infected compartment
θ	**0.000104***	Estimated	The rate at which asymptomatic infected individuals become symptomatic infected
ϕ	**0.00567***	Estimated	The rate at which symptomatic infected become treated
γ_A	0.0714	(35)	The recovery rate for asymptomatic infected individuals
γ_S	0.042	(35)	The recovery rate for symptomatic infected individuals
γ_T	0.0714	Assumed	The recovery rate for treated individuals
δ	0.0011	Calculated	The rate at which recovered individuals become susceptible (loss rate of immunity)

Results

Basic Reproduction Number

The basic reproduction number,R_0, represents the average number of secondary infections generated by a single infected individual in a fully susceptible population. Utilizing the parameter values presented in Table 3, we calculated the mean R_0 to be 6.010. Since R_0 >1, this result indicates that the model is not asymptotically stable, suggesting that the disease will persist over time. Furthermore, Table 3 illustrates the variations in R_0 under different parameter values, offering additional insights into its dynamic behaviour. This high value suggests persistent transmission potential under current conditions. It does not align with (44)'s findings that diphtheria's basic reproduction number can fall below one (R0 < 1), indicating the potential for the disease to fade out over time if current control measures are sustained.

Table 3 Basic Reproduction Number

	Varying Values		
Parameter	1	**2**	3
β_1	0.0201	0.201	0.901
β_p	0.0503	0.503	1.503
β_v	0.095	0.95	1.95
γ_A	0.00714	0.0714	0.714
β_2	0.00709	0.0709	0.709
γ_s	0.0042	0.042	0.42
θ	0.0000104	0.000104	0.00104
μ_1	0.0011	0.011	0.11
μ	0.00000491431	0.0000491431	0.00491431
λ_u	50	100	150
ω	0.00114	0.0114	0.114
z	0.000777	0.00777	0.0777
τ	0.00289	0.0289	0.289
ε	0.0007	0.0707	0.707
α	0.0146	0.146	0.546
ϕ	0.000567	0.00567	0.0567
ρ	0.02	0.2	0.9
$\mathbf{R_0}$	0.5417901752	5.785074823	11.70305638
Mean $\mathbf{R_0}$		**6.010**	

Sensitivity of Basic Reproduction Number

The sensitivity analysis of the basic reproduction number (R_0) provides crucial insights into the factors that most influence diphtheria transmission dynamics. The findings, as shown in Table 4, indicate that the asymptomatic infection transmission rate (β_1), symptomatic infection transmission rate (β_2), the rate at which susceptible individuals become partially vaccinated (β_P), the rate at which susceptible individuals become fully vaccinated (β_V), natural death rate (μ), diphtheria-induced death rate (μ_1), the recovery rate for asymptomatic infected individual (γ_A), the recovery rate for symptomatic infected individual (γ_S), recruitment rate (λ_u), the rate at which fully vaccinated individuals become susceptible (ω), the rate at which partially vaccinated individuals become susceptible (z), the rate at which individuals go from being fully vaccinated to partially vaccinated (τ), the rate at which partially vaccinated individuals become fully vaccinated (ε), proportion of infectious population (ρ), rate of progression from the exposed class to either the asymptomatic compartment or the infected compartment (α), the rate at which asymptomatic infected individuals become symptomatic infected (θ), and the rate at which symptomatic infected become treated (ϕ)have the tendency to influence the spread of diphtheria.

The asymptomatic infection transmission rate (β_1), symptomatic infection transmission rate (β_2), recruitment rate (λ_u), natural death rate (μ), rate of progression from the exposed class to either the asymptomatic compartment

or the infected compartment (α), the rate at which fully vaccinated individuals become susceptible (ω), the rate at which partially vaccinated individuals become susceptible (z), the rate at which individuals go from being fully vaccinated to partially vaccinated (τ), and the rate at which partially vaccinated individuals become fully vaccinated (ε) are positively sensitive parameters that can significantly elevate R_0, exacerbating the spread of diphtheria.

Conversely, the rate at which susceptible individuals become partially vaccinated (β_P), the rate at which susceptible individuals become fully vaccinated (β_V), diphtheria-induced death rate (μ_1), the recovery rate for asymptomatic infected individual (γ_A), the recovery rate for symptomatic infected individual (γ_S), proportion of infectious population (ρ), the rate at which asymptomatic infected individuals become symptomatic infected (θ), and the rate at which symptomatic infected become treated (ϕ) are negatively sensitive and can significantly reduce R_0, thus minimizing the spread of diphtheria.

Table 4: Sensitivity indices of R_0 to the model parameters

Parameters	Value	Sensitivity Index
β_1	0.201	0.8892
β_p	0.503	-0.1909
β_v	0.95	-2.1178
γ_A	0.0714	-0.7695
β_2	0.0709	0.1108
γ_s	0.042	-0.0792
θ	0.000104	-0.0006
μ_1	0.011	-0.1585
μ	0.0000491431	0.0053
ϕ	0.00567	-0.0107
ρ	0.2	-0.1122
λ_u	100	1.0000
α	0.5611	0.0193
τ	0.0289	0.2011
z	0.00777	0.2870
ε	0.0707	0.8356
ω	0.0114	0.9196

Effect of Transmission Rate on the Spread of Diphtheria

Figure 2 highlights the central role of asymptomatic transmission in driving disease spread by examining the effects of varying the asymptomatic infection transmission rate (β_1) across key population compartments under three different values: low (β_1 = 0.0201), moderate (β_1 = 0.201), and high (β_1 = 0.901), representing increasing levels of transmission from individuals without clinical symptoms. As shown in Figure 2 (a), higher values of (β_1) lead to a much faster depletion of the susceptible population.

When asymptomatic transmission is low, the susceptible pool declines gradually, reflecting limited spread. However, even moderate increases in (β_1) substantially accelerate this decline, while high asymptomatic transmission rapidly exhausts the susceptible population. The exposed compartment [Figure 2 (b)] shows a similar pattern. Low asymptomatic transmission results in slow growth of exposed individuals, whereas moderate and high (β_1) values produce increasingly rapid increases. At high (β_1), the exposed population rises sharply and early, indicating widespread silent transmission and rapid seeding of new infections before symptoms appear. Figures 2 (c) and 2(d) further show that increases in (β_1) strongly amplify both asymptomatic and symptomatic infections. Higher asymptomatic transmission drives a steep rise in the asymptomatic infected population and, indirectly, fuels symptomatic cases through continued community spread. Figure 2 (e) shows that higher (β_1) values lead to a much larger recovered population over time, reflecting extensive transmission throughout the community.

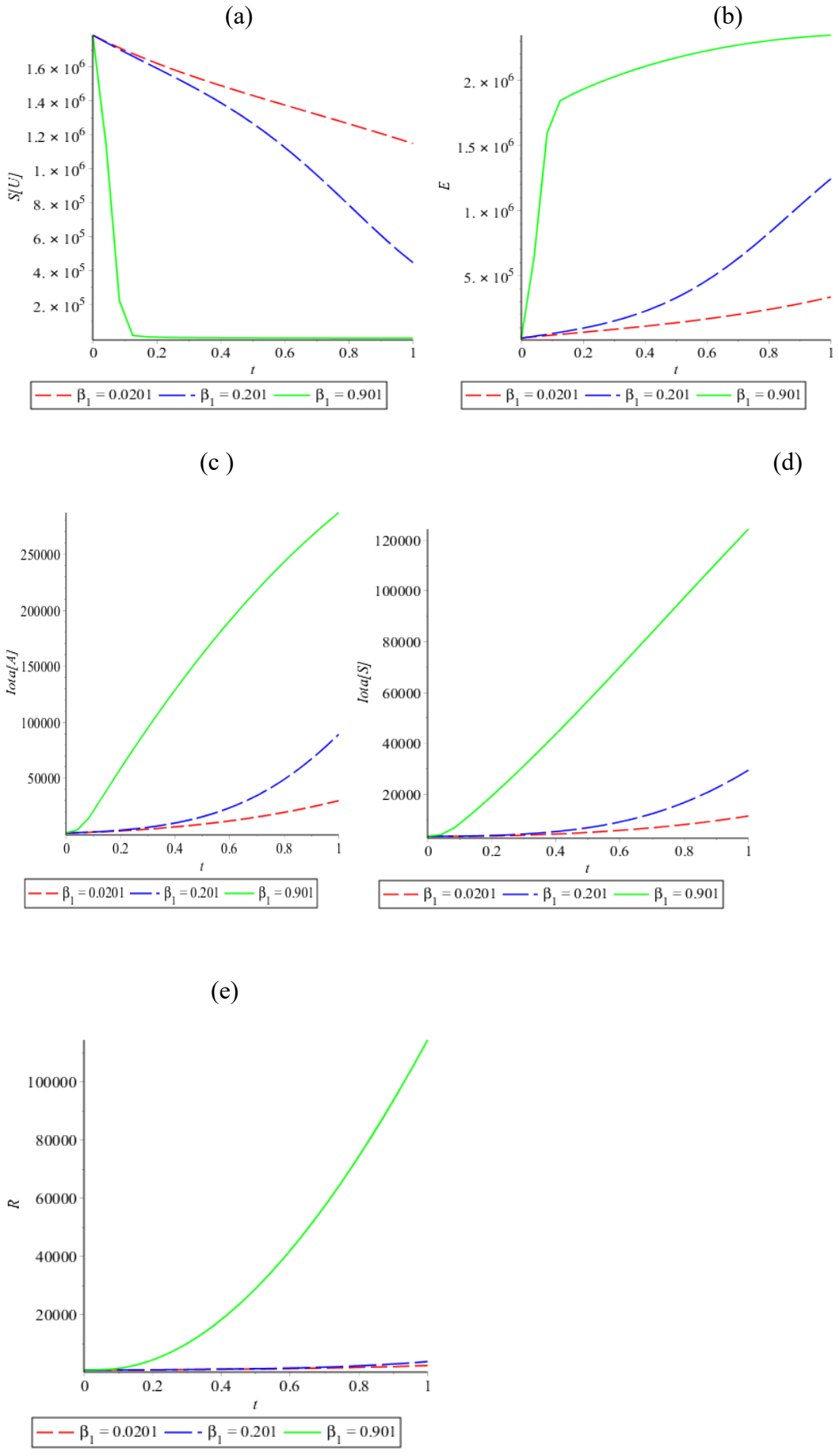

Figure 2: Effect of Asymptomatic Infection Transmission Rate on the Spread of Diphtheria based on different Compartments at time (t) in weeks: (a) Susceptible compartment; (b) Exposed compartment; (c) Asymptomatic compartment; (d) Symptomatic compartment; (e) Recovered compartment.

Figure 3 illustrates how changes in the symptomatic infection transmission rate (β_2) influence the progression of the epidemic across multiple population compartments under three different values: low (β_2 = 0.00709), moderate (β_2 = 0.0709), and high (β_2= 0.709) to capture increasing levels of transmission from symptomatic individuals. As shown in Figure 3 (a), higher values of (β_2) lead to a much faster decline in the susceptible population. When symptomatic transmission is low, the susceptible pool decreases slowly, indicating limited spread. However, even moderate increases in (β_2) markedly accelerate the loss of susceptibles, while high transmission rapidly depletes this compartment, driving it toward near-zero levels. This highlights the strong influence of symptomatic individuals on the speed and scale of disease spread. The exposed compartment [Figure 3 (b)] responds sharply to changes in (β_2). Low symptomatic transmission results in only a modest rise in exposed individuals, whereas moderate and high values produce increasingly rapid growth. At high (β_2), exposure rises steeply before leveling off, suggesting that a large fraction of the population becomes exposed in a short period. Figures 3(c) and (d) show that higher (β_2) amplifies both asymptomatic and symptomatic infections. Increased symptomatic transmission indirectly fuels asymptomatic cases through greater overall exposure, while symptomatic infections themselves grow in a strongly nonlinear manner, with high (β_2) producing near-exponential increases. Figure 3 (e) indicates that higher (β_2) leads to a faster and larger accumulation of recovered individuals, reflecting the downstream effect of widespread infection.

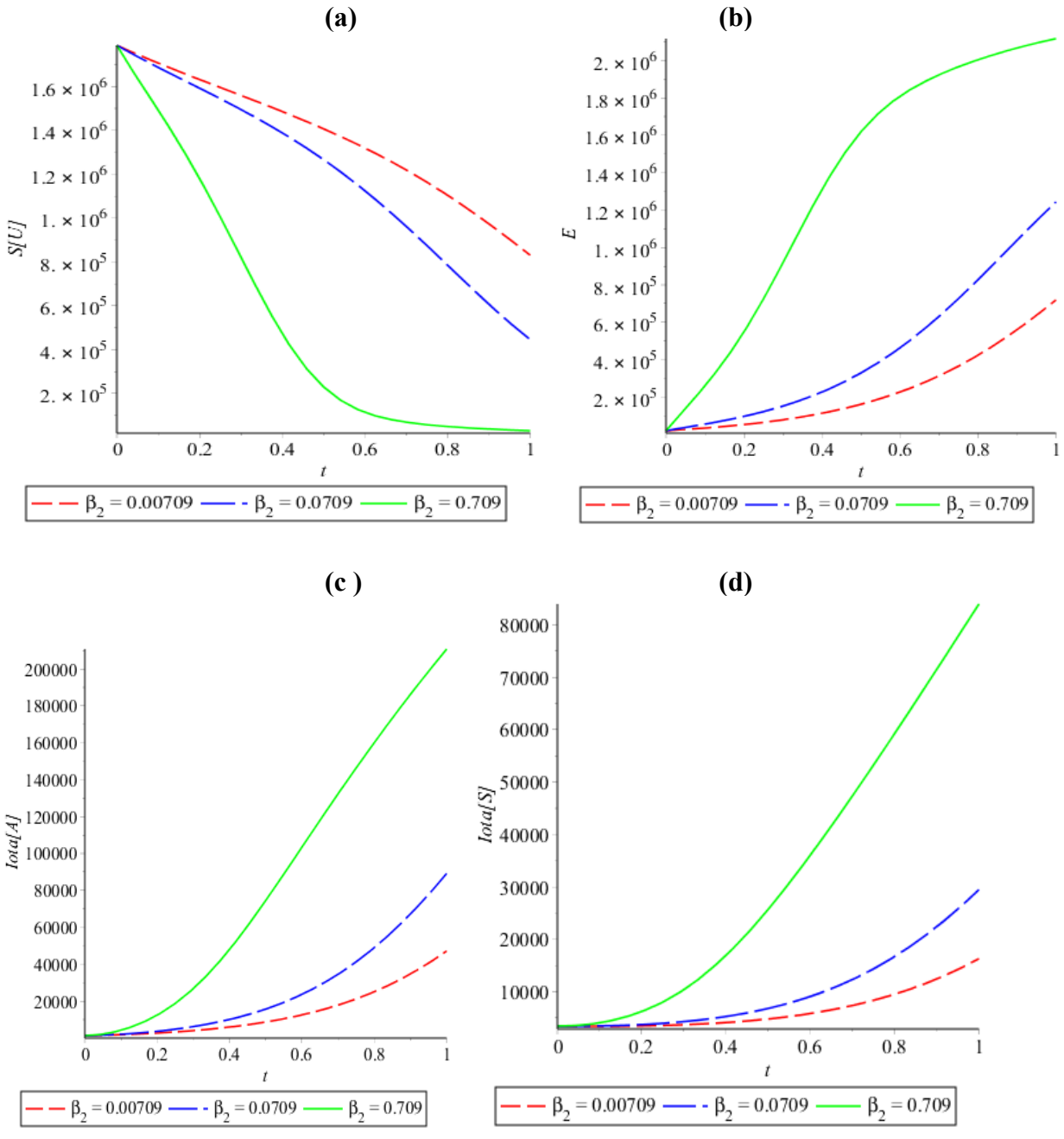

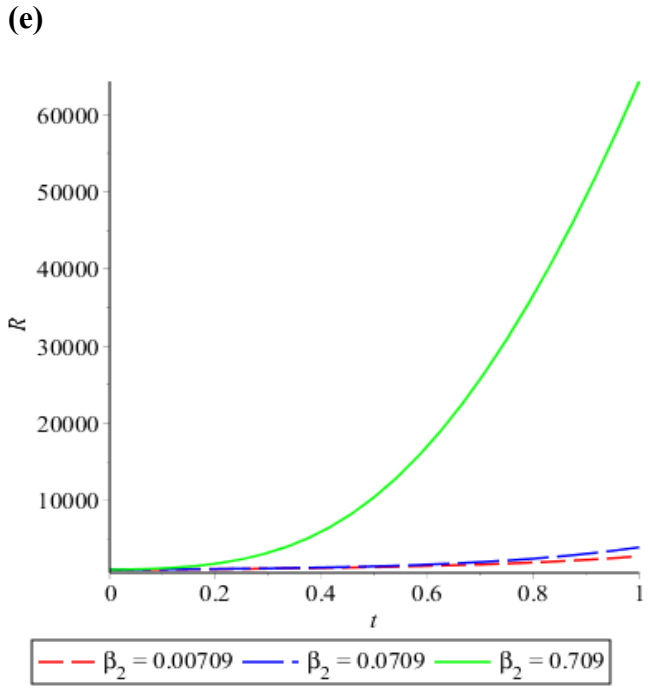

Figure 3: Effect of Symptomatic Infection Transmission Rate on the Spread of Diphtheria based on different Compartments at time (t) in weeks: (a) Susceptible compartment; (b) Exposed compartment; (c) Asymptomatic compartment; (d) Symptomatic compartment; (e) Recovered compartment.

Effective Vaccination Scenario

Effective vaccination is determined using the rate at which susceptible individuals become fully vaccinated (β_V) and the rate at which partially vaccinated individuals become fully vaccinated. Figure 4 illustrates the impact of the rate at which susceptible individuals become fully vaccinated (β_V) on both the susceptible and fully vaccinated compartments over time under three different vaccination values: low (β_V = 0.15), moderate (β_V = 0.95), and high (β_V = 1.75) are considered to assess how vaccination intensity influences epidemic control. Figure 4 (a) shows that increasing (β_V) leads to a more rapid decline in the susceptible population. At low vaccination rates, the reduction in susceptibles is gradual, leaving a large portion of the population vulnerable for an extended period. In contrast, moderate and high values of (β_V) produce a steeper decrease, with the highest vaccination rate resulting in a swift depletion of the susceptible compartment. Figure 4 (b) further indicates that higher values of (β_V) significantly increase the size of the fully vaccinated compartment. As (β_V) rises, the number of fully vaccinated individuals grows more rapidly and stabilizes at a higher level over time.

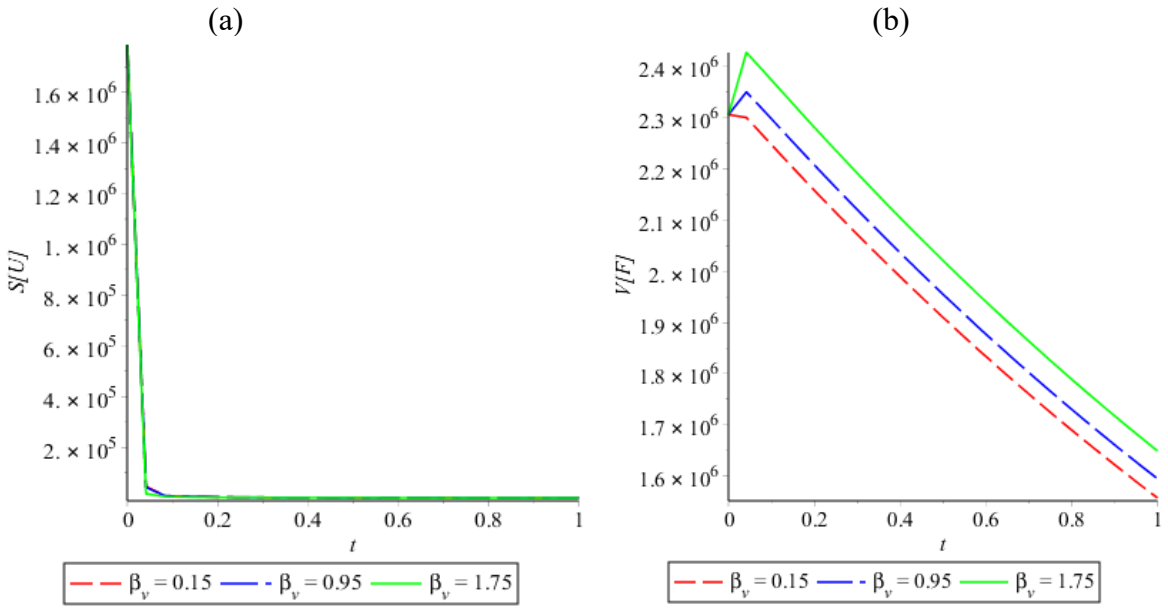

Figure 4: Effect of the rate at which susceptible individuals become fully vaccinated (β_V) at time (t) in weeks: (a) Susceptible compartment; (b) Fully Vaccinated compartment

Figure 5 shows how quickly moving people from partial to full vaccination influences overall protection in the population. When the transition rate (ε) is low, many individuals remain vulnerable for longer periods, slowing the reduction in susceptibility. As (ε) increases to moderate and high levels, the number of unvaccinated susceptible individuals drops much faster. Notably, the outcomes for moderate and high rates are very similar, suggesting that once vaccination schedules are completed promptly, further acceleration provides only limited additional benefit. The effect on the fully vaccinated population is particularly evident [Figure 5 (a)]. At low and moderate transition rates, the number of fully vaccinated individuals increases only slightly before declining, reflecting slow movement into full protection and the impact of waning immunity. In contrast, a high transition rate leads to a rapid buildup of fully vaccinated individuals, creating a stronger but temporary boost in population immunity. This highlights that fast completion of vaccination schedules can substantially improve short-term protection, although maintaining this benefit requires continued vaccination efforts. Changes in the partially vaccinated compartment further emphasize this point [Figure 5 (b)]. When progression to full vaccination is slow, partially vaccinated individuals accumulate and remain in this intermediate state. With faster transition rates, this group shrinks steadily as people move more quickly to full vaccination.

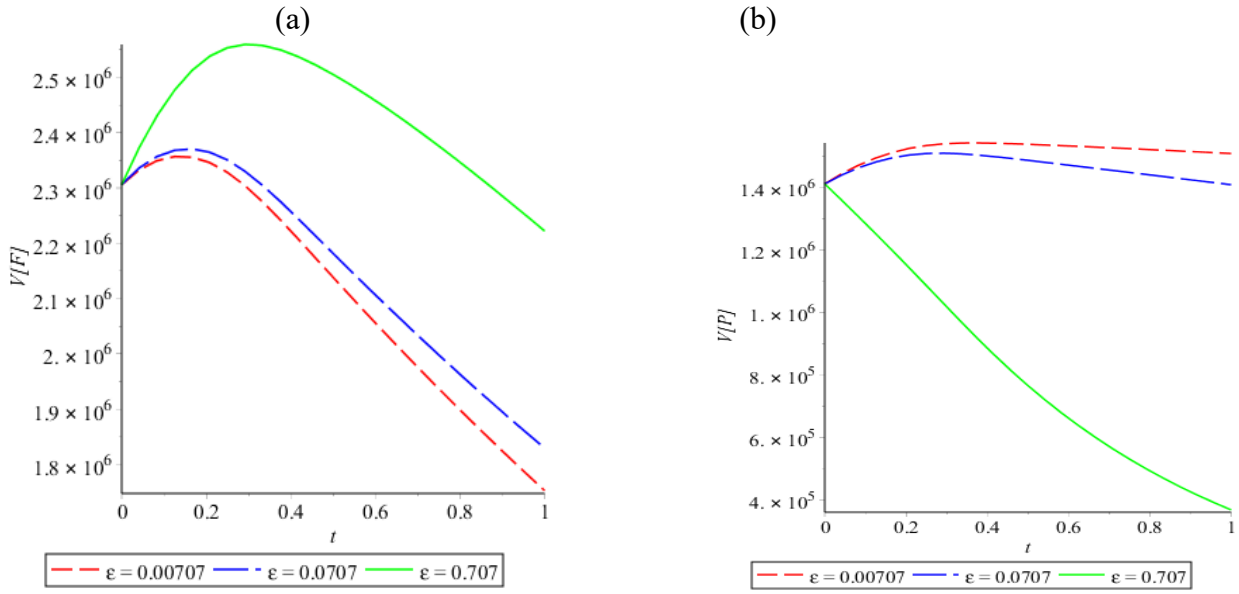

Figure 5: Effect of the Rate at which Partially Vaccinated Individuals become Fully Vaccinated (ε) on Diphtheria Prevalence at time (t) in weeks: (a) Fully Vaccinated compartment: (b) Partially Vaccinated compartment

Ineffective Vaccination Scenario

Ineffective vaccination is determined by the rate at which partially vaccinated individuals become susceptible (z) on the susceptible compartment. Figure 6 illustrates how the rate at which partially vaccinated individuals lose their protection and return to susceptibility (Z) influences both the susceptible and partially vaccinated populations under three different values: low (Z = 0.000777), moderate (Z = 0.0777), and high (Z = 0.777) to capture varying degrees of loss of partial immunity. Figure 6 (a) shows that when loss of partial protection is slow, the susceptible population declines rapidly and remains relatively low over time, indicating that partial vaccination continues to provide meaningful protection. As (Z) increases, this decline becomes much slower, leading to a larger pool of susceptible individuals. At high values of (Z), partial immunity wanes quickly, allowing many individuals to re-enter the susceptible class and increasing vulnerability to infection. Figure 6 (b) highlights the corresponding effects on the partially vaccinated compartment. At low (Z), the number of partially vaccinated individuals grows steadily, reflecting sustained retention of partial immunity. In contrast, high reversion rates cause a sharp decline in this compartment, as individuals rapidly lose protection and transition back to susceptibility. Moderate values of (Z) produce intermediate behaviour between these extremes.

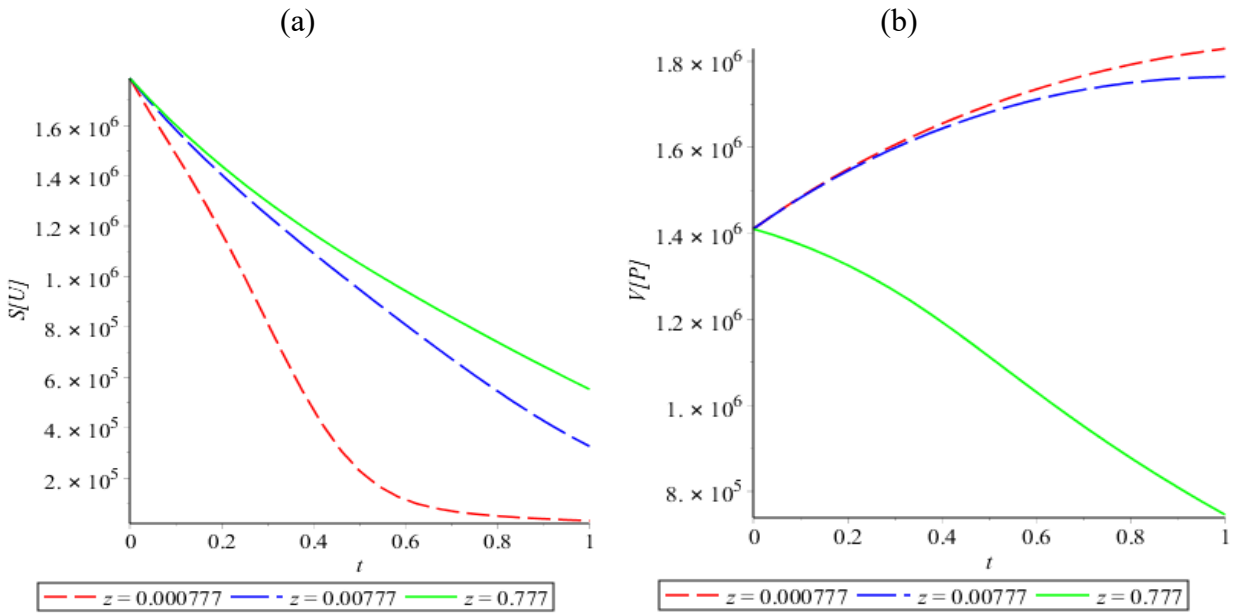

Figure 6: Effect of the Rate at which Partially Vaccinated Individuals become Susceptible (Z) on Diphtheria Prevalence at time (t) in weeks: (a) Susceptible Compartment; (b) Fully Vaccinated Compartment.

Incomplete vaccination

The incomplete vaccination is determined by the rate at which susceptible individuals become partially vaccinated. Figure 7 demonstrates how the rate at which susceptible individuals become partially vaccinated affects the susceptible compartment over time. The curves display three different values of the effect: 0.103 (red dashed), 0.503 (blue dashed), and 0.903 (solid green), representing low, moderate, and high levels, respectively.

Figure 7 (a) shows how increasing the rate at which susceptible individuals receive a partial vaccine dose changes the course of the diphtheria infection. When partial vaccination occurs slowly, many people remain fully susceptible for a long time. As the rate of partial vaccination increases, the susceptible population shrinks much faster, indicating that even a single vaccine dose can quickly reduce the number of people at highest risk of infection. At the highest uptake level, this reduction happens early and sharply, underscoring the value of rapidly expanding access to initial vaccination. The effects are also evident in the partially vaccinated compartment [Figure 7 (b)]. Higher partial vaccination rates lead to more people entering this compartment early on, resulting in a higher and more sustained peak. In contrast, lower vaccination rates result in fewer partially vaccinated individuals and a quicker decline over time. This pattern suggests that strong early uptake of partial vaccination not only reduces vulnerability but also maintains a meaningful level of intermediate protection in the population.

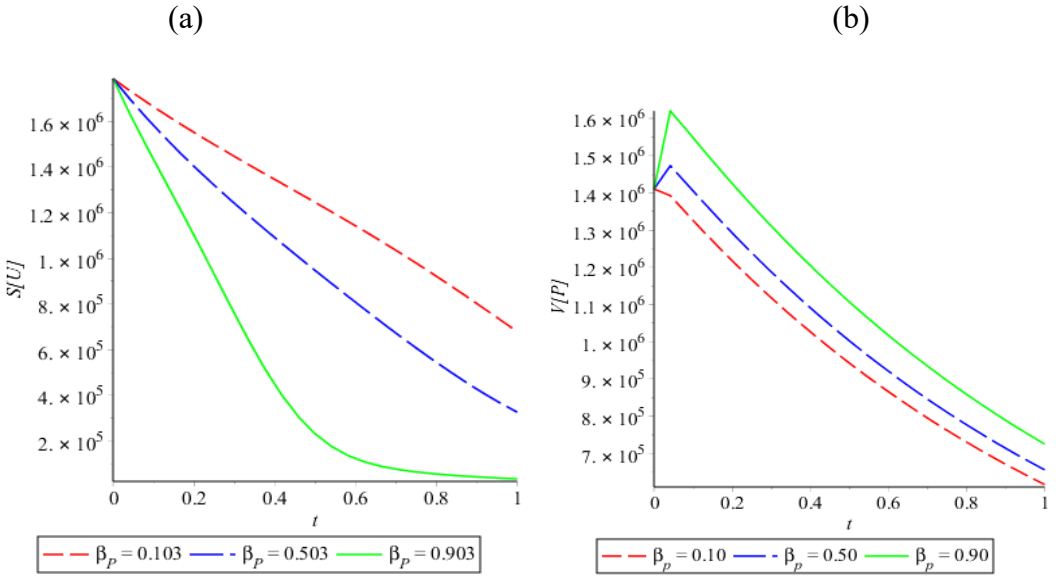

Figure 7: Effect of the Rate at which Susceptible Individuals become Partially Vaccinated (β_P) on Diphtheria Prevalence at time (t) in weeks: (a) Susceptible Compartment; (b) Partially Vaccinated Compartment.

Vaccine Waning Scenario

Figure 8 illustrates how the rate at which fully vaccinated individuals lose immunity and return to susceptibility (ω) affects both the susceptible and fully vaccinated compartments under three different values: low (ω = 0.00114), moderate (ω = 0.0114), and high (ω = 0.114) to reflect different levels of durability of vaccine-induced immunity. Figure 8 (a) shows that when immunity wanes slowly, the susceptible population declines rapidly and remains relatively small, indicating strong and lasting vaccine protection. As (ω) increases, this decline becomes much slower, and the susceptible pool remains larger over time. At high rates of immunity loss, vaccinated individuals return more quickly to susceptibility, sustaining vulnerability within the population. This highlights the importance of durable vaccine-induced immunity in effectively reducing the number of people at risk. Figure 8 (b) further demonstrates that (ω) strongly shapes the fully vaccinated compartment. At low and moderate values, the fully vaccinated population grows and is maintained at high levels, reflecting long-lasting protection. In contrast, when (ω) is high, the fully vaccinated population increases only briefly before declining steadily, signaling a rapid loss of immunity. Together, these results emphasize that faster waning of full vaccine protection undermines long-term vaccination benefits.

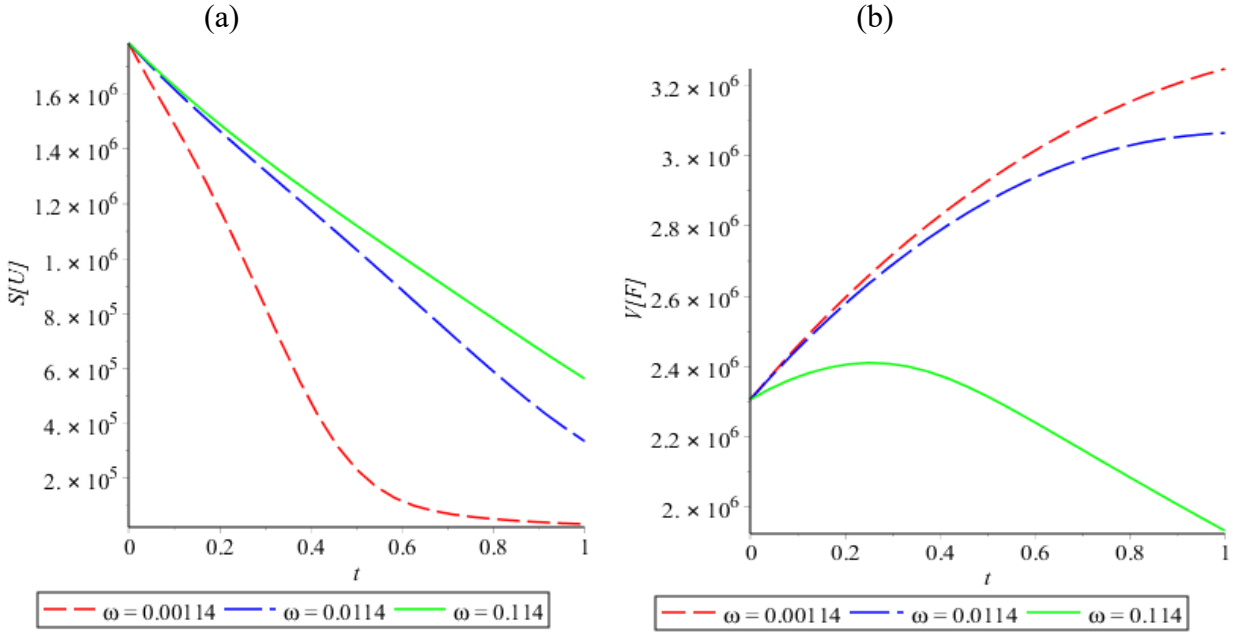

Figure 8: Effect of the Rate at which Fully Vaccinated Individuals become Susceptible (ω)on Diphtheria Prevalence at time (t) in weeks: (a) Susceptible Compartment; (b) Fully Vaccinated Compartment

Treatment Scenario

Figure 9 illustrates how the recovery rate of treated individuals (γ_T) shapes the progression of infection and recovery across multiple compartments under three different values: low (γ_T = 0.00714), moderate (γ_T = 0.0714), and high (γ_T = 0.714) to capture differences in treatment effectiveness.

Figure 9a shows that higher recovery rates among treated individuals slow the growth of asymptomatic infections. When recovery is rapid, fewer individuals remain infectious for extended periods, leading to lower levels of asymptomatic cases over time. In contrast, slow recovery allows infections to persist longer, resulting in a faster and larger accumulation of asymptomatic individuals. This indicates that effective treatment can indirectly reduce silent transmission within the population. A similar pattern is observed for symptomatic infections in Figure 9 (b). As (γ_T) increases, the number of symptomatic cases grows more slowly and reaches much lower peak levels. Low recovery rates are associated with sustained and higher symptomatic burdens, whereas high recovery rates substantially suppress symptomatic prevalence. This highlights the critical role of timely and effective treatment in limiting disease severity and spread.

The impact on the treatment compartment is shown in Figure 9 (c). When recovery is slow or moderate, individuals accumulate in treatment, leading to a rapidly growing treatment burden. In contrast, a high recovery rate results in a much slower increase, as patients exit treatment more quickly. Figure 9 (d) demonstrates that faster recovery dramatically accelerates the rise in the recovered

population, contributing to earlier buildup of population immunity.

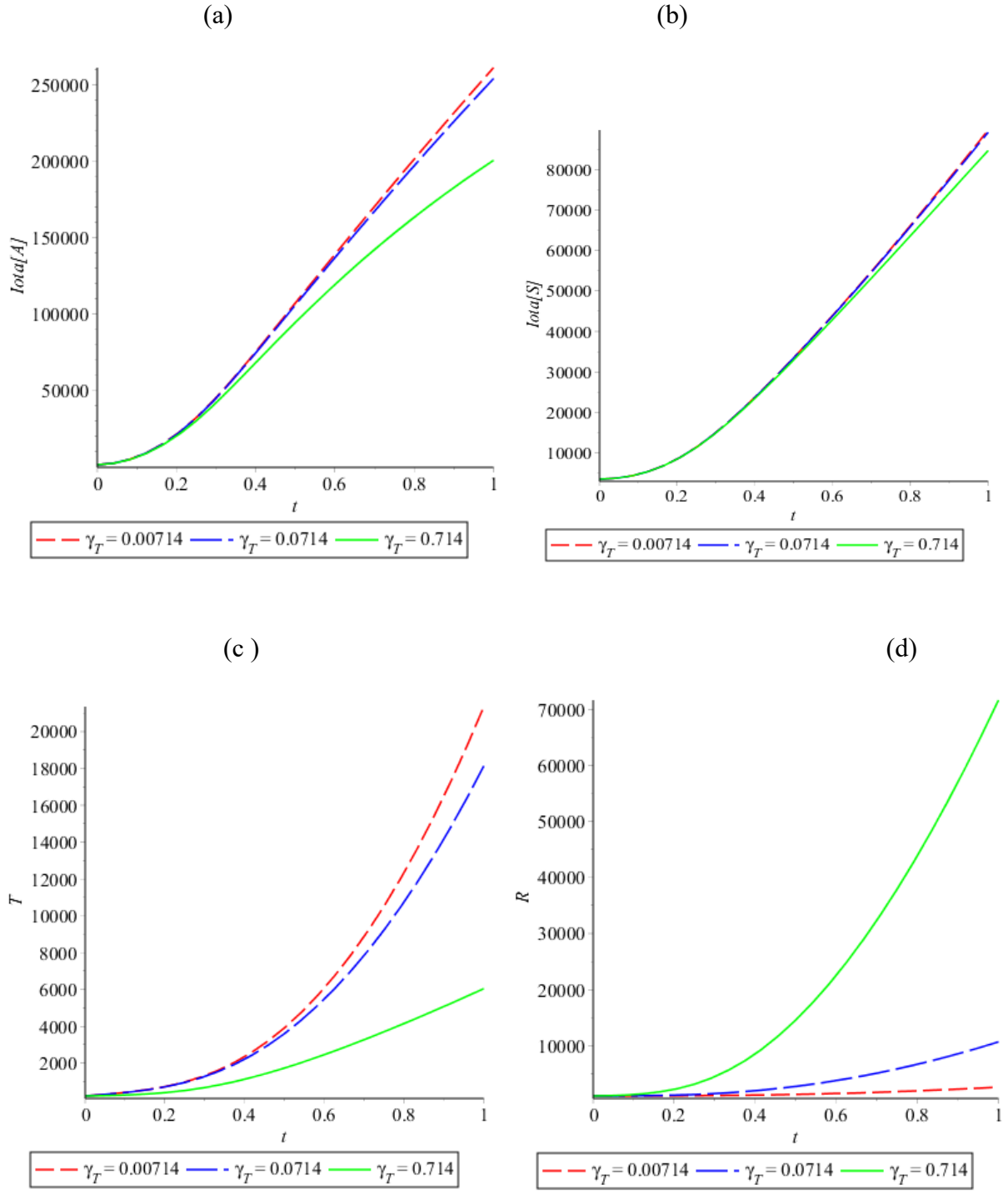

Figure 9: Effect of the Recovery Rate for Treated Individuals(γ_T) on the Spread of Diphtheria at time (t) in weeks: (a) Asymptomatic Infected Compartment; (b) Symptomatic Infected Compartment; (c) Recovered Compartment; (d) Treatment Compartment.

Discussion of Results

The results from Figures. 1 and 2 clearly show that both asymptomatic and symptomatic transmission drive diphtheria spread, with asymptomatic transmission emerging as a particularly powerful yet often overlooked contributor. Our findings align with growing evidence that asymptomatic individuals sustain transmission for extended periods, enabling quiet spread before detection(34,44,45). As the asymptomatic transmission rate increases, the susceptible population declines rapidly, while the exposed compartment surges, in line with (44), who demonstrated that even modest asymptomatic transmission accelerates epidemic growth.

Similarly, (29,34) showed how silent transmission undermines strategies focused solely on isolating symptomatic cases. Higher symptomatic transmission

rates produce comparable effects: rapid depletion of susceptibles, sharp rises in exposed and infected compartments, and disproportionately large epidemic responses, even from small increases (29,34). Symptomatic cases also indirectly amplify asymptomatic infections by boosting overall exposure (44). Meanwhile, elevated asymptomatic transmission leads to a large recovered population, reflecting uncontrolled spread and widespread recovery at the cost of larger outbreaks (45). Although recovery builds immunity, it often arises reactively rather than through prevention, underscoring the limitations of symptom-only controls.

Figures 3 and 4 demonstrate vaccination's central role in curbing transmission, through both high coverage and schedule completion. Faster transitions from susceptible to fully vaccinated states shrink the at-risk pool, consistent with studies emphasizing vaccination's reliability for diphtheria control (7,28,30,35,37,38,45). Slow progression from partial to full vaccination leaves many partially protected and transmission-competent (4,29,34). Notably, moderate and high completion rates yield similar susceptibility reductions, suggesting diminishing returns beyond reasonable timelines (28,34,46).

Figures 5 and 6 underscore the partial vaccination's important but limited protective effect. Faster first-dose uptake reduces the fully susceptible pool, providing short-term risk reduction, especially early in outbreaks when full schedules are impractical (32,34,44,45,47). Low uptake sustains high vulnerability, while higher rates mimic first-dose campaigns that curb spread pre-full coverage.

Figures 7 and 8 reveal waning immunity's strong influence on long-term dynamics. Low waning rates sustain small susceptible pools and large fully vaccinated compartments, ensuring durable control (31,34,45). Higher rates replenish susceptibles, enabling persistent transmission despite coverage (29,44). Gradual shifts from full to partial vaccination at higher waning rates leave individuals with incomplete protection, insufficient against infection or onward spread (28,34,45).

Figure 9 illustrates that a faster recovery from treatment suppresses both asymptomatic and symptomatic infections by shortening infectious periods, alleviating healthcare burdens, and accelerating population recovery. This aligns with evidence on rapid case management's transmission-interrupting effects (28,29,34,35,44,45).

This study has several notable strengths, including a comprehensive compartmental model that explicitly incorporates asymptomatic and symptomatic transmission, multiple vaccination states (unvaccinated, partially vaccinated, and fully vaccinated), waning immunity, and treatment dynamics, enabling a realistic depiction of diphtheria transmission and control. Extensive sensitivity analyses across numerical solutions further bolster robustness by pinpointing key drivers, such as recruitment rate, waning rate from fully vaccinated individuals to susceptibles, asymptomatic infection transmission rate, and waning rate from partially vaccinated individuals to susceptibles.

However, limitations include the assumption of homogeneous mixing, which overlooks spatial heterogeneity and behavioural factors such as vaccine hesitancy, health system constraints, and uncertainties in adherence. Future research should integrate stochastic and spatial models alongside optimal control strategies to jointly optimize vaccination, boosters, and treatment under resource constraints, and to target measures against asymptomatic carriers.

Conclusion

In this study, we developed a diphtheria vaccine-treatment model with eight compartments: Susceptible (unvaccinated) population (S_U), fully vaccinated (V_F), partially vaccinated (V_P), exposed (E), asymptomatic infected (I_A), symptomatic infected (I_S), treated (T), and recovered (R). The calculated basic reproduction number (R_0) was found to be greater than 1, indicating that, under current conditions, diphtheria is likely to increase over time unless control measures are improved. Sensitivity analysis identified drivers of (R_0), highlighting the critical role of certain parameters in sustaining and suppressing the spread of diphtheria. The model shows that recruitment rate, waning rate from fully vaccinated individuals to susceptibles, asymptomatic infection transmission rate, and waning rate from partially vaccinated individuals to susceptibles significantly contribute to disease spread. The evaluation of intervention

strategies shows that vaccination, especially rapid progression to full coverage, is the most effective intervention. Partial vaccination and waning immunity underscore the need for timely booster programs and sustained coverage. Rapid treatment and recovery further suppress transmission and reduce healthcare burdens. This study emphasizes the necessity of comprehensive vaccination strategies, vigilant monitoring of asymptomatic transmission, and rapid treatment to achieve and sustain diphtheria elimination.

Conflicts of Interest: "The authors declare no conflict of interest including financial or non-financial interests."

References

1. World Health Organization. Disease Outbreak News; Diphtheria in Nigeria. 2023 Oct 18;
2. Nigeria Centre for Disease Control. Diphtheria Situation Report, Serial Number 03, Data as at Epi-week 31: An Update on Diphtheria Outbreak in Nigeria. 2023;
3. Elsinga J, van Meijeren D, Reubsaet F. Surveillance of diphtheria in the Netherlands between 2000–2021: cutaneous diphtheria supersedes the respiratory form. BMC Infect Dis. 2023 Jun 21;23(1):420.
4. Kanchanarat S, Chinviriyasit S, Chinviriyasit W. Mathematical Assessment of the Impact of the Imperfect Vaccination on Diphtheria Transmission Dynamics. Symmetry (Basel). 2022 Sep 24;14(10):2000.
5. Medugu N, Musa-Booth TO, Adegboro , B., Onipede AO, Babazhitsu M, Amaza R. A review of the current diphtheria outbreaks. African Journal of Clinical and Experimental Microbiology. 2023 Apr 18;24(2):120–9.
6. Marshall NC, Baxi M, MacDonald C, Jacobs A, Sikora CA, Tyrrell GJ. Ten Years of Diphtheria Toxin Testing and Toxigenic Cutaneous Diphtheria Investigations in Alberta, Canada: A Highly Vaccinated Population. Open Forum Infect Dis. 2022 Jan 1;9(1).
7. Sornbundit K, Triampo W, Modchang C. Mathematical modeling of diphtheria transmission in Thailand. Comput Biol Med. 2017 Aug;87:162–8.
8. Besa NC, Coldiron ME, Barki A, Raji A, Nsuami MJ, Rousseau C, et al. Diphtheria outbreak with high mortality in northeastern Nigeria. Epidemiol Infect. 2014 Apr 18;142(4):797–802.
9. Yang Y, Zhang H. Mathematical Models and Control Methods of Infectious Diseases. In: 2020 5th International Conference on Automation, Control and Robotics Engineering (CACRE). IEEE; 2020. p. 383–8.
10. White PJ. Mathematical Models in Infectious Disease Epidemiology. In: Infectious Diseases. Elsevier; 2017. p. 49-53.e1.
11. Swart EM, van Gageldonk PGM, de Melker HE, van der Klis FR, Berbers GAM, Mollema L. Long-Term Protection against Diphtheria in the Netherlands after 50 Years of Vaccination: Results from a Seroepidemiological Study. PLoS One. 2016 Feb 10;11(2):e0148605.
12. Bansiddhi H, Vuthitanachot V, Vuthitanachot C, Prachayangprecha S, Theamboonlers A, Poovorawan Y. Seroprevalence of Antibody Against Diphtheria Among the Population in Khon Kaen Province, Thailand. Asia Pacific Journal of Public Health. 2015 Mar 28;27(2):NP2712–20.
13. Huppert A, Katriel G. Mathematical modelling and prediction in infectious disease epidemiology. Clinical Microbiology and Infection. 2013 Nov;19(11):999–1005.
14. Kurugöl Z, Midyat L, Türkoğlu E, İşler A. Immunity against diphtheria among children and adults in Izmir, Turkey. Vaccine. 2011 Jun;29(26):4341–4.
15. Gamboa M, Lopez-Herrero M. Measures to assess a warning vaccination level in a stochastic SIV model with imperfect vaccine. Studies in Applied Mathematics. 2022 May 4;148(4):1411–38.
16. Hethcote HW. The Mathematics of Infectious Diseases. SIAM Review. 2000 Jan 1;42(4):599–653.
17. Kretzschmar M, Wallinga J. Mathematical Models in Infectious Disease Epidemiology. In 2009. p. 209–21.
18. Akpan EA, Ikono FG, Udom CF, Umondak UJ, Ikeh OH, Nyong EG. UNDERREPORTING IN INFECTIOUS DISEASE CASES: A TIME SERIES REGRESSION-SIR APPROACH. Jurnal Biometrika dan Kependudukan. 2025 Jul 11;14(1):22–33.
19. Mirsaeedi F, Sheikhalishahi M, Mohammadi M, Pirayesh A, Ivanov D. Compartmental models in epidemiology: bridging the gap with operations research for enhanced epidemic control. Ann Oper Res. 2025 Oct 20;
20. Reyné B, Saby N, Sofonea MT. Principles of mathematical epidemiology and compartmental modelling application to COVID-19. Anaesth Crit Care Pain Med. 2022 Feb;41(1):101017.
21. Prodanov D. Analytical solutions and parameter estimation of the SIR epidemic model. In: Mathematical Analysis of Infectious Diseases. Elsevier; 2022. p. 163–89.
22. Kiseleva O, Yakovlev S, Prytomanova O, Kuzenkov O. Mathematical Modeling of Regional Infectious Disease Dynamics Based on Extended Compartmental Models. Computation. 2025 Aug 4;13(8):187.
23. Pathak S, Kota VR. Mathematical Analysis of an Infectious Disease Model: Stability, Persistence, and Equilibrium Analysis in a Non-Linear Epidemiological System. Journal of Nonlinear Mathematical Physics. 2025 Oct 6;32(1):64.
24. Ozsahin DU, Khan NA, Aqeel A, Ahmad H, Alotaibi MF, Ayaz M. Mathematical modeling and dynamics of immunological exhaustion caused by measles transmissibility interaction with HIV host. PLoS One. 2024 Apr 18;19(4):e0297476.
25. Khumbudzo M, Duah E, Grobler E, Maluleke K. The Role of Mathematical Modelling in Predicting and Controlling Infectious Disease Outbreaks in Underserved Settings: A

Systematic Review and Meta-Analysis. Public Health Challenges. 2025 Sep 13;4(3).
26. Greening B, Meltzer MI. 24 Mathematical Modeling for Emergency Response: Using Models to Inform and Direct Response Priorities and Shape the Research Agenda. In: Principles and Practice of Emergency Research Response. Cham: Springer International Publishing; 2024. p. 645–67.
27. Kretzschmar ME, Ashby B, Fearon E, Overton CE, Panovska-Griffiths J, Pellis L, et al. Challenges for modelling interventions for future pandemics. Epidemics. 2022 Mar;38:100546.
28. Andrawus J, Omotoso KI, Andrew AA, Eguda FY, Babuba S, Ibrahim KG. Mathematical model analysis on the significance of surveillance and awareness on the transmission dynamics of diphtheria. Journal of the Nigerian Society of Physical Sciences. 2025 Nov 1;2618.
29. Djaafara BA, Adrian V, Eriawati E, Elyazar IRF, Hamers RL, Baird JK, et al. Modeling the transmission dynamics and control strategies during the 2017 diphtheria outbreak in Jakarta, Indonesia. Infect Dis Model. 2025 Mar;11(1):1–15.
30. Akponana E, Egbune N, Akindele O. Mathematical Modelling of Diphtheria Transmission Dynamics for Effective Strategies of Prevention and Control with Emphasis on Impact of Vaccination and Waning Immunity. International Journal of Research in Engineering and Science. 2024 Jul;12(7):142–53.
31. Olayiwola MO, Alaje AI. Mathematical modelling of diphtheria transmission and vaccine efficacy using Nigeria. Model Earth Syst Environ. 2024 Jun 8;10(3):3941–67.
32. Izzati N, Yannuansa N, Ummah I, Wati DAR, Indahwati E, Purwasih SM, et al. Dynamical analysis of a mathematical model on the spread of diphtheria disease with vaccination completeness factors. Journal Focus Action of Research Mathematic (Factor M). 2024 Dec 31;7(2):206–23.
33. Amalia P, Toaha S. Optimal Control of Mathematical Model of Diphtheria Spreading. Daya Matematis: Jurnal Inovasi Pendidikan Matematika. 2022 Jun 24;10(2):138.
34. Gourram H, Baroudi M, Sahib I, Labzai A, Herradi K, Belam M. Mathematical modeling and strategy for optimal control of diphtheria. Results in Control and Optimization. 2024 Dec;17:100481.
35. Madubueze CE, Tijani KA, Fatmawati. A deterministic mathematical model for optimal control of diphtheria disease with booster vaccination. Healthcare Analytics. 2023 Dec;4:100281.
36. Musa S, Usaini S, Ahmed I, Kiataramkul C, Tariboon J. Dynamics of the Diphtheria Epidemic in Nigeria: Insights from the Kano State Outbreak Data. Mathematics. 2025 Apr 4;13(7):1189.
37. Oguntolu FA, Peter OJ, Omede BI, Balogun GB, Ajiboye AO, Panigoro HS. Mathematical Modeling on the Transmission Dynamics of Diphtheria with Optimal Control Strategies. Jambura Journal of Biomathematics (JJBM). 2025 Mar 29;6(1):1–22.
38. Getachew FZ, Teklu SW, Alemneh HT. Optimal control and economic evaluation of diphtheria disease model with booster immunization and hospitalization. Sci Rep. 2025 Oct 27;15(1):37517.
39. Wiah EN, Otoo H, Nabubie IB, Mohammed HR. Nonlinear Dynamics and Chaos in HIV/AIDS Epidemic Model with Treatment. Applied Mathematics. 2014;4(3):86–96.
40. Akpan EA, Udom CF, Mukhtar FM. Next-Generation Matrix Approach for Computing the Basic Reproduction Number of Infectious Diseases. Math Methods Appl Sci. 2025 Dec 22;48(18):16888–98.
41. Mukhtar FM, Lasisi KE, Rasheed BA, Akpan EA, Udom CF. Sensitivity Analysis of Transmission Parameters in A Diphtheria-Vaccine-Treatment Model. Journal of the Royal Statistical Society Nigeria Group (JRSS-NIG Group). 2025 Nov 28;2(2):407–29.
42. Powell D, Fair J, LeClaire RJ, Moore LM, Thompson D. Sensitivity Analysis for an Infectious Disease Model. International System Dynamics Conference, Boston, MA. 2005;
43. Chitnis N, Hyman JM, Cushing JM. Determining Important Parameters in the Spread of Malaria Through the Sensitivity Analysis of a Mathematical Model. Bull Math Biol. 2008 Jul 22;70(5):1272–96.
44. Sahib I, Baroudi M, Khajji B, Faouzi L, Alia M, Herradi K, et al. Modeling and predicting the spread of diphtheria in guinea using delayed stochastic differential equations. Communications in Mathematical Biology and Neuroscience. 2024 Dec 5;Vol 2024(Article ID 134).
45. Chebotaeva V, Srinivasan A, Vasquez PA. Differentiating Contact with Symptomatic and Asymptomatic Infectious Individuals in a SEIR Epidemic Model. Bull Math Biol. 2025 Mar 4;87(3):38.
46. Truelove SA, Keegan LT, Moss WJ, Chaisson LH, Macher E, Azman AS, et al. Clinical and Epidemiological Aspects of Diphtheria: A Systematic Review and Pooled Analysis. Clinical Infectious Diseases. 2020 Jun 24;71(1):89–97.
47. Wu Z, Lin L, Zhang J, Zhong J, Lai D. Global burden of diphtheria, 1990–2021: a 204-country analysis of socioeconomic inequality based on SDI and DTP3 vaccination differences before and after the COVID-19 pandemic (GBD 2021). Front Public Health. 2025 Jun 20;13.
48. Reverte V, Zornoza-Moreno M, Molina-Salas YE, Romera-Guirado FJ, Celdrán-Navarro MDC, Pérez-Martín JJ. Does a correlation exist between delayed vaccination and a decreased vaccine confidence? Hum Vaccin Immunother. 2024 Dec 31;20(1).